J Mater Sci (2007) 42:4801–4809
DOI 10.1007/s10853-006-0748-6

Modulus spectroscopy of lead potassium titanium niobate ($Pb_{0.95}K_{0.1}Ti_{0.25}Nb_{1.8}O_6$) ceramics

Konapala Sambasiva Rao · Prayaga Murali Krishna · Dasari Madhava Prasad · D. Gangadharudu

Received: 23 February 2006 / Accepted: 1 August 2006 / Published online: 19 March 2007

Abstract The modulus Spectroscopy of Lead Potassium Titanium Niobate ($Pb_{0.95}K_{0.1}Ti_{0.25}Nb_{1.8}O_6$, PKTN) Ceramics was investigated in the frequency range from 45 Hz to 5 MHz and the temperature, from 30 to 600 °C. XRD analysis in PKTN indicated a orthorhombic structure with lattice parameters a = 18.0809 Å, b = 18.1909 Å and c = 3.6002 Å. The dielectric anomaly with a peak was observed at 510 °C. Variation of ε^{I} and ε^{II} with frequency at different temperatures exhibit high values, which reflects the effect of space charge polarization and/or conduction ion motion. The electrical relaxation in ionically conducting PKTN ceramic analyzed in terms of Impedance and Modulus formalism. The Cole–Cole plots of impedance were drawn at different temperatures. The dielectric modulus, which describes the dielectric relaxation behaviour is fitted to the Kohlrausch exponential function. Near the phase transition temperature, a stretched exponential parameter β indicating the degree of distribution of the relaxation time has a small value. From the AC conductivity measurements the activation energy near phase transition temperature (T_C°C) has been found to different from that of the above and below T_C. The temperature dependence of electrical modulus has been studied and results are discussed.

K. S. Rao (✉) · P. M. Krishna · D. M. Prasad · D. Gangadharudu
Centre for Piezoelectric Transducer Materials, Physics Department, Andhra University, Visakhapatnam 530 003, India
e-mail: konapala@sify.com

Introduction

Lead Potassium Niobate ($Pb_{(1-x)}$ $K_{2x}Nb_2O_6$, PKN at x = 0.2) is a useful substrate material for surface acoustic wave devices [1, 2] .It has a largest electromechanical coupling factors K_{15} = 0.69 and K_{24} = 0.73 [3] . PKN belongs to the orthorhombic structure with space group C_{2v}^{14}–Cm2m at room temperature and Curie temperature, 450 ± 10 °C. Substitution of Lead by Gd in PKN ($Pb_{2(1-x)}Gd_xK_{1+x}Nb_5O_{15}$) and its structural modification for different values of x have been reported by Oualla et al. [4]. It has been reported that the charge carriers in PKN ceramics were coupled with the soft mode mechanism [5, 6].

Impedance spectroscopy has been widely used for investigating the properties of electric materials and electrochemical synthesis. The aims of impedance measurements are the identification of physical processes and the determination of various electrical properties appropriate for the electrical system under study. It requires the selection of a model suitable with the measurement data. The commonly used models are electrical equivalent circuits consisting of resistors, capacitors, inductors, and specialized distributed elements. The basic information about the dielectric properties of materials can be obtained from the complex impedance analysis. The impedance analysis allows the separation of several contributions of total impedance, arising from the bulk conductance and interfacial phenomenon viz. grain, grain boundary and other electrode interface effects. The data may be analyzed in terms of four possible complex formalisms, the impedance Z*, the electrical modulus M*, the admittance A* (or Y*) and the permittivity (ε*). The relation among the above properties are given by [7],

$$M^* = J\omega C_0 Z^*$$

$$\varepsilon^* = (M^*)^{-1}$$

$$A^* = (Z^*)^{-1}$$

$$A^* = J\omega C_0 \varepsilon^*$$

where $\omega = 2\pi f$, is angular frequency, C_0 is vacuum capacitance of the measuring cell and electrodes with air gap equal to the thickness of sample.

In this paper we measured the frequency dependence of dielectric constant, impedance, electrical modulus and AC conductivity at different temperatures. Using the electric modulus representation the conductivity behavior of PKTN ceramic has been characterized over wide range of frequencies and temperatures. The frequency dispersion of conductivity, conduction mechanism and electrical relaxation processes at different temperatures are explained.

Experimental procedure

The ceramic specimen $Pb_{0.95}K_{0.1}Ti_{0.25}Nb_{1.8}O_6$ (PKTN) was prepared by the conventional technique of milling, pre-firing, crushing and sintering. Analar grade PbO, K_2CO_3, TiO_2 and Nb_2O_5 were used as raw materials. These raw materials were weighed according to the formula given above. The weighed powders were mixed in methanol and then calcined at about 900 °C/4 h. This calcination procedure was repeated thrice to achieve homogeneous with single-phase composition. After calcination the ceramic powder has been pressed into pellets with 12 mm in diameter and 2 mm in thickness and then sintered at 1110–1150 °C for 60 min. The ceramic was polished and electroded with silver paste. The dielectric constant, dielectric loss, impedance and modulus parameters were measured using a computer interfaced HIOKI 3532-50 LCR Hi-TESTER. The crystal structure of the material PKTN has been determined from the Philips X-Ray diffractometer using Cu K_α radiation.

Results and discussion

Structure

Figure 1 shows the X-ray diffractogram of PKTN. The 100% intensity peak in PKN ($Pb_{1-x}K_{2x}Nb_2O_6$) for $x = 0.20$, 0.23, 0.26, 0.29 0.32 and 0.34 has been observed at around $2\theta = 32°$, which was found to be the characteristic feature of the composition. In the present PKTN material the 100% intensity peak is observed at $2\theta = 29.635°$. The shift in 2θ of 100% intensity peak may be attributed to the presence of, 2θ may be attributed to the presence of titanium.

The composition PKTN has been confirmed as a single phase with Orthorhombic structure by indexing all the peaks by Interpretation and Indexing program by E. Wu, School of physical Sciences, Flinders University of South Australia, Bed ford park, Australia. The lattice parameters a, b and c were computed. The computed values of a, b, c, cell volume (Å^3), experimental density ($d_{\text{expt.}}$), X-Ray density ($d_{\text{theo.}}$), percentage of density, porosity and orthorhombic distortion were given in Table 1.

It is evident from the table that the lattice parameters $a = 18.080$ Å, $b = 18.190$ Å and $c = 3.600$ Å were found to be much higher when compared with PKN [8]

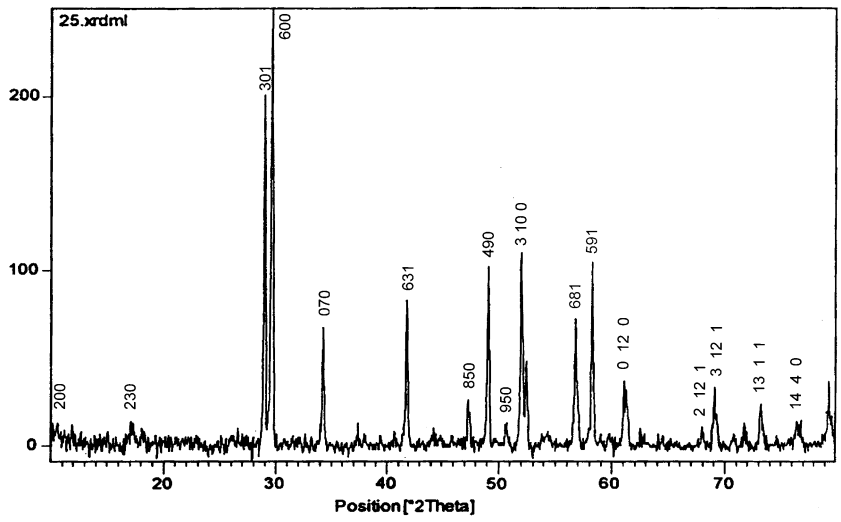

Fig. 1 X-ray diffractogram of PKTN sample

Table 1 Lattice parameters of PKTN

Composition	Lattice parameters (Å)	Cell volume (Å^3)	Ortho-rhombic distortion (b/a)	Density (g/cm^3)		Porosity	% Density
				$d_{theo.}$	$d_{expt.}$		
PKTN	a = 18.0809 b = 8.1909 c = 3.6002	1184.13	1.006	6.67	6.29	0.005	94.3

at $x = 0.20$–0.34. The enhancement in the lattice parameters may be due to the higher content of Pb present in PKTN. Also, the percentage of density achieved in PKTN is more than 94% indicating the material having a good density. The orthorhombic distortion (b/a = 1.006) obtained in the material is very small indicating a minute change in Pb content leads to the tetragonal phase of PKN [9].

Dielectric

The real dielectric constant of PKTN as a function of temperature at different frequencies is shown in Fig. 2. The dielectric anomaly has been found at 510 °C. The Curie point of Pb-K-Niobates shows strong dependence on x. The dependence of x on T_C can be represented by an empirical relationship as

$$T_C = 570 - (97.488)x - (2498)x^2$$

Here, the value of $x = 0.05$, then from the above equation T_C is found to be 558.88 °C. The experimental value of T_C found to be lower than the theoretical one. The reason being Niobium is partially substituted with Titanium and the empirical relation is not taken into account of B—cation substitutions. The lower value of T_C = 510 °C may be due to the presence of Titanium.

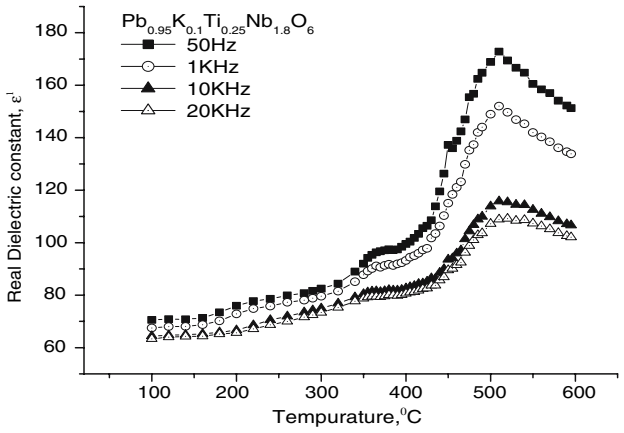

Fig. 2 Real dielectric constant of PKTN ceramic as a function of temperature

Table 2 Dielectric data

Composition	PKTN
ε^{I}_{RT}	81.47
T_C (°C)	510
ε^{I}_{TC}	152
K (×10^5)	1.20

It is observed that the room temperature dielectric constant (ε_{RT}) be 82 and the dielectric constant at transition temperature (ε_{TC}) as 152. Further, the Curie temperature T_c is found to be independent of frequencies, which reveals that PKTN belong to normal ferroelectric material. The Curie–Weiss law has been obeyed in para region and Curie–Weiss constant has been calculated and found to be 1.20×10^5. From the value of Curie constant (K) one can conclude that the present material PKTN belongs to oxygenocatahedra ferroelectric [10, 11]. The values ε_{RT} , ε_{TC}, K and T_c are tabulated in Table 2.

Figure 3 shows the variation of real and imaginary dielectric constant (ε^I and ε^{II}) with frequency at different temperatures (350–590 °C), which includes ferroelectric and paraelectric region of PKTN material. The value of ε^I and ε^{II} at 45 Hz is nearly same at measured temperature of 350 °C. As the temperature increases the values of ε^I and ε^{II} differs and intersects at lower frequency. Further, increase in temperature the intersection of ε^I and ε^{II} moves towards higher frequency side i.e., 480 °C onwards. As the temperature increases the magnitude of ε^I with frequency also decreases and flatten. Both ε^I and ε^{II} rise sharply towards low frequencies and the shape of the raise is changes as the temperature increases. The sharp raise of ε^I and ε^{II} at low frequencies may be due to the conducting ion motion. Also, ε^I and ε^{II} exhibit high values, which reflects the effect of space charge polarization and/or conduction ion motion. In the conducting dielectric materials the high values of ε^I may be interpreted as accumulation of charges at the interface between sample and electrode i.e., space charge polarization. Regarding the high value of ε^{II} at low frequency may be due to free-charge motion with in the material and/or related to AC conductivity relaxation [12].

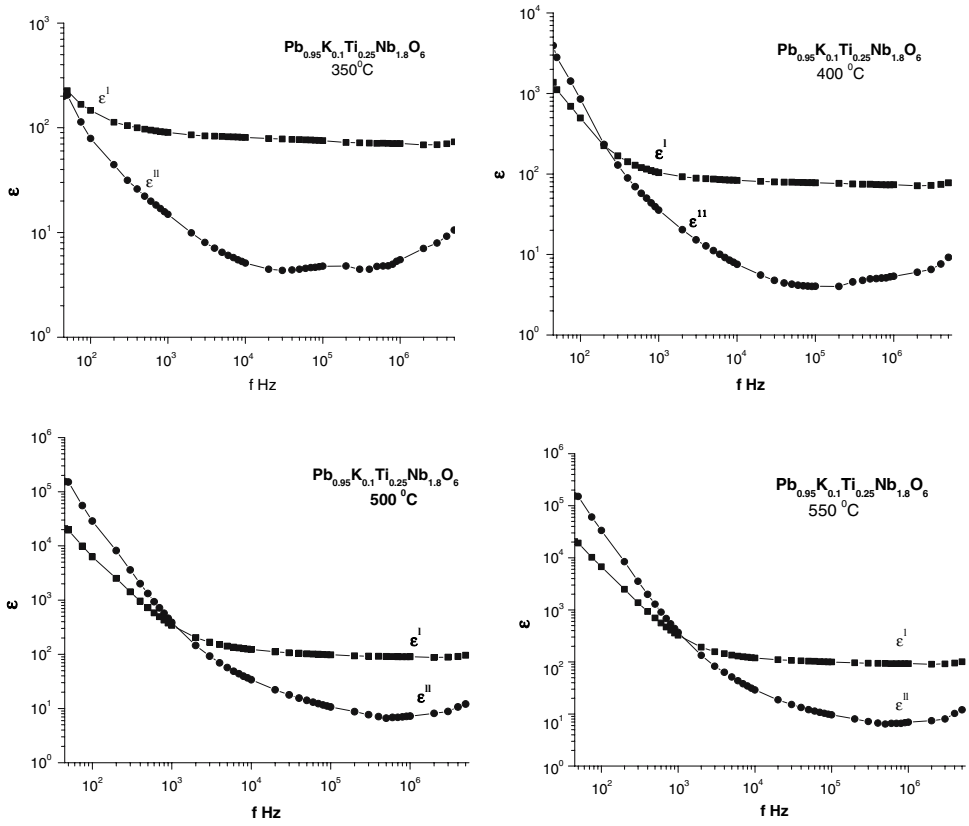

Fig. 3 Variation of real and imaginary dielectric constant (ε^{I} and ε^{II}) with log f at different temperatures

Impedance characterization

Electrical properties of electroceramics at fixed frequency don't give a whole set of properties towards the evaluation of the electric parameters as a function of temperature. Electroceramic materials gives a variety of frequency dependent phenomena associated with grain boundaries region and intrinsic properties of material [13–15]. Impedance spectroscopy studies allowed us the measurements under wide range of frequencies which will be useful to separate the contributions of electroactive regions viz, grain boundary and grain (bulk).

Argand diagrams, imaginary part of complex impedance Z* versus its real part allow us the determination of the bulk ohmic resistance as a function of temperature and there by temperature dependence of the conductivity [16, 17]. A single arc approximating a semicircle has been observed at low temperatures in PKTN. Figure 4. shows variation of Z with log f at 510 °C and corresponding Argand diagram. It is evident from the Fig. 4a that Z^{I} intersects Z^{II} at a particular frequency indicating the existence of relaxation phenomena. As the temperature increases the intersection frequency of Z^{I} with Z^{II} shifts towards high frequency side reveals the shift in relaxation frequency.

Figure 5 shows Cole–Cole plots of impedance in PKTN at several (300–590 °C) temperatures. It is evident from figures that at lower temperatures Z^{II} increase with increase of Z^{I} indicating the insulating behavior of the material. Below 400 °C a straight-line response has been observed. As the temperature

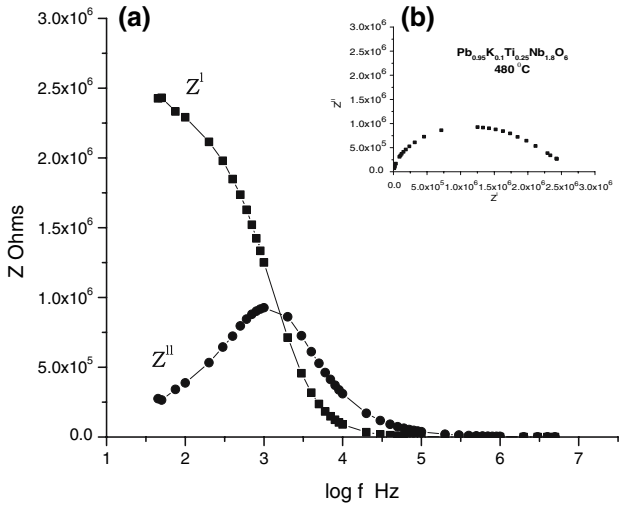

Fig. 4 (**a**) Frequency dependence of Z^{I} and Z^{II} (**b**) corresponding Argand diagram

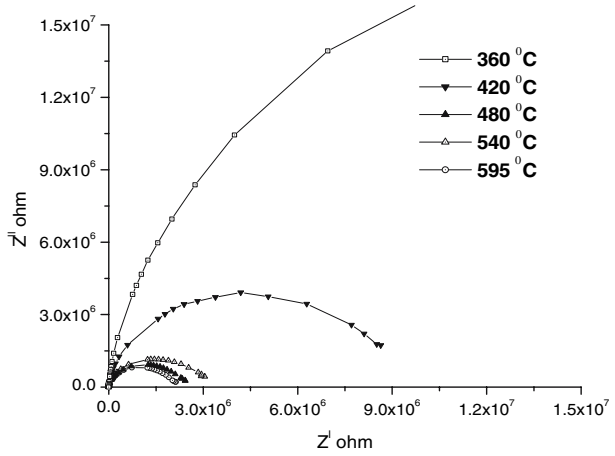

Fig. 5 Cole–Cole Plots of PKTN

increases the slope of the line decreases and which makes a curve towards real axis. Temperature above 400 °C the curve becomes almost semi-circle indicating the increase in conductivity of the sample.

All the impedance plots in PKTN exhibits the phenomena of decentralization, in which the centers of semi-circles that compose the total electric response centered below the real axis making an angle (Φ) with *x*-axis. It has been observed that the value of Φ is found to increase with increase in temperature at the transition temperature the value of Φ is maximum, further increase in temperature results decrease in the value of Φ. In addition, it has been observed that the shape of the diagram (Fig. 6) suggests that the electrical response is composed of overlapping of two semi-circles. Also, the high overlapping degree suggests that each contribution presents very similar relaxation frequency ($\omega = 2\pi f$). The small semi circles definition is assigned to very similar values of most relaxation frequency, with relation each relaxation phenomenon detected, one to grain and other to grain boundary. Therefore, the overlapping increases with decreasing

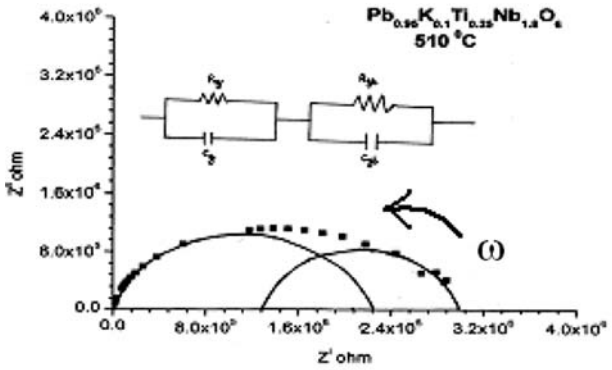

Fig. 6 Impedance diagram of PKTN and its equivalent circuit

of magnitude of the difference between the most relaxation frequencies.

The width of the overlapping decreases with increase in temperature. The electric and dielectric properties of PKTN are well represented by two parallel RC elements in series. The first relaxation phenomenon was observed at lower frequencies represent the grain boundary contribution to the electrical response. The second one, in the high frequency range was observed, corresponds to specific properties of grain or bulk.

From the Cole–Cole plots, the grain and grain boundary resistances and capacitances at various temperatures have been calculated. Variation of resistance (grain resistance, R_g and grain boundary resistance, R_{gb}), capacitance (grain capacitance, Cg and grain boundary capacitance, C_{gb}), grain relaxation time and grain boundary relaxation time with temperature in PKTN have been shown in fig 7(a–c). It is evident from the fig. 7 (a) that the value of grain resistance is found to be higher compare with grain boundary resistance. Also, an anomaly in R_{gb} has been found at 565–570 °C. From Fig. 7b the value of grain capacitance has been found to be higher when compare with grain boundary capacitance. A similar anomaly in grain boundary capacitance has also been observed at 565 °C. It is evident from Fig. 7c that the grain relaxation time is higher than the grain boundary relaxation time.

Variation of grain, grain boundary conduction and relaxation time with inverse temperature shows Arrhenius behavior, and the corresponding grain (E_g eV), grain boundary (E_{gb} eV) conduction, grain relaxation activation energy (ε_g eV) and grain boundary relaxation activation energy (ε_{gb} eV) values have been calculated. These values are tabulated in Table 3. From the above discussion one can conclude that the conducting parameter in PKTN is probably due to grain boundary.

Modulus characterization

Dielectric relaxation studies in PKTN have been carried out at temperatures between 240 and 595 °C in the complex modulus M* formulation. Figure 8a, b shows the real and imaginary parts of the electrical modulus, M^I and M^{II} as a function of frequency at various temperatures. At 240 °C the value of M^I shows 1.7×10^{-3} at 45 Hz. This value has been decreased with increase in temperature. As frequency increases value of M^I increases and reaches a constant value at higher frequencies, this trend is nearly the same at all temperatures under study. At low frequency M^I approaches zero (Fig. 8a) confirming the presence of

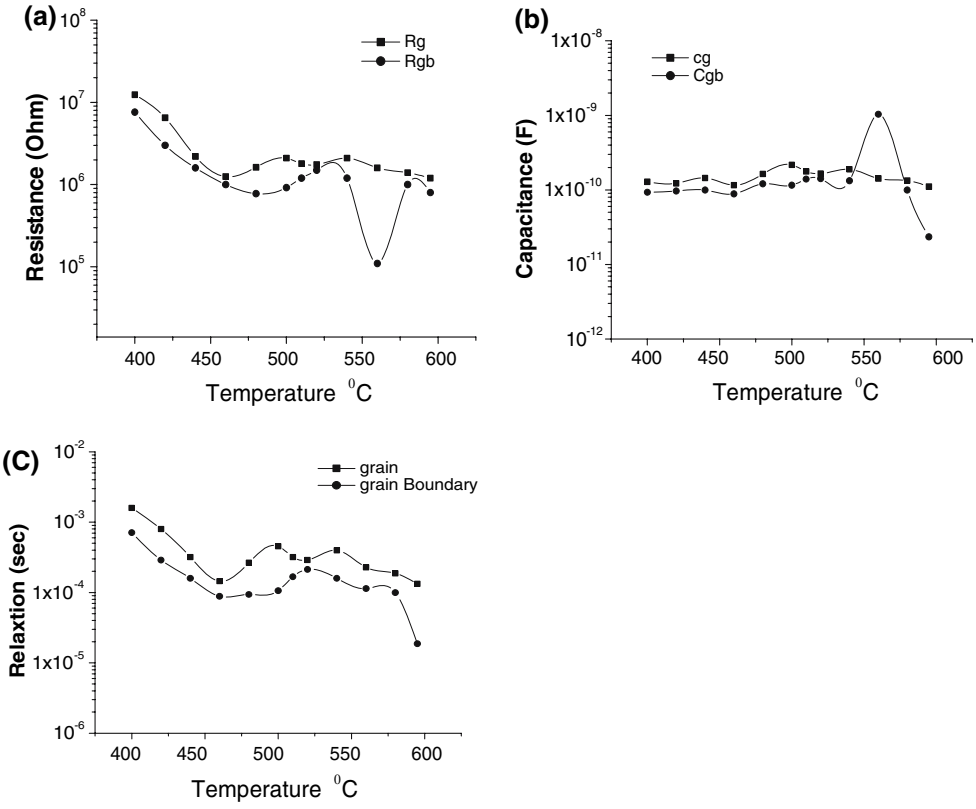

Fig. 7 (**a**–**c**) variation of resistance, capacitance and relaxation of grain and grain boundary with temperature

Table 3 Conduction and relaxation activation energy values (eV) for grain and grain boundary

Temperature range (°C) PKTN	Grain conduction activation energy, E_g (eV)	Grain boundary conduction activation energy, E_{gb} (eV)	Grain relaxation activation energy, ε_g (eV)	Grain boundary relaxation activation energy, ε_{gb} (eV)
580–515	0.16	0.14	0.82	0.69
510–430	0.45	0.50	0.31	0.57

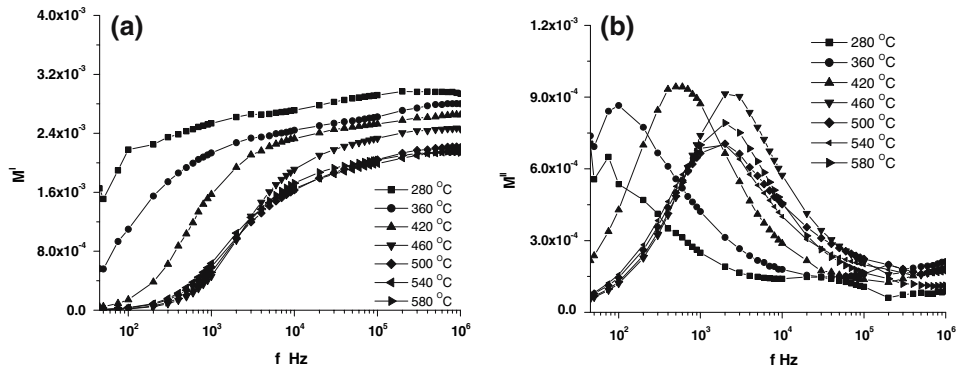

Fig. 8 (**a**, **b**) Variation of Real and imaginary part of electrical modulus M^I and M^{II} as function of frequency at various temperatures

an appreciable electrode and/or ionic polarization in the temperature range under investigation. The real part of modulus M^I has a value of zero at low frequency and increases with increase in frequency, and the dispersion shifts towards high frequency as temperature increases (Table 4).

It is evident from the Fig. 8b that there is a shift in the peak frequencies of M^{II} to high frequency side as temperature increases. Increasing temperature, the dc conduction is attributed to long-range motion of ions that are thermally activated. The low frequency side of the peak represents the range of frequency in which the ions can move long ranges i.e., ions can perform successfully hopping from one site to the neighboring site. The high frequency side of the M^{II} represents the range of frequencies in which the ions are separately

Table 4 Activation energy (eV) values for PKTN

Composition	PKTN			
Temperature Range (°C)	Activation energy (eV)			
	20 K	10 K	1 K	500 Hz
250–410	0.075	0.081	0.2	0.19
420–520	0.24	0.23	0.42	0.42
525–590	0.12	0.12	1.58	1.58

confined to their potential wells, and the ion can make only the localized motion within the wells [18–21]. Also, M^{II} peak frequencies increases with increase in temperature and the shift in frequency of M^{II} peaks corresponds to the so called conductivity relaxation. The activation energy of dc conduction can be obtained from Arrhenius plots of M^{II} peak frequencies. The reciprocal of frequency of the M^{II} peak represents the time scale of the transition from the long-range mobility and is identified as the characteristics relaxation time. Above and below the phase transition temperature of PKTN two distinct slopes of activation energy (1.50 eV, 0.43 eV) obtained from the Arrhenius plot were found, which corresponds the dc activation energy i.e., the ionic hopping mechanism.

Figure 9 shows the dc conductivity obtained from impedance Cole–Cole plot in the temperature range 400–595 °C, which covers the transition temperature of the sample. The dc conductivity was estimated from bulk resistance, which was derived from the equivalent circuit model in the complex impedance plots of a resistor and capacitor in parallel. It is evident from the figure that near the phase transition temperature, two activation energies (1.60 eV, 0.45 eV) were obtained from Arrhenius plots.

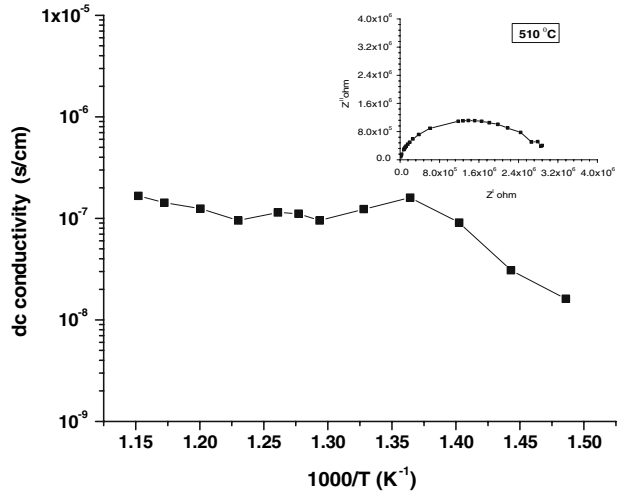

Fig. 9 DC conductivity obtained from impedance Cole–Cole plot as a function of 1/T

Figure 10 shows the temperature dependency of AC conductivity at various frequencies. Activation energies are calculated and are given in table. Near phase transition temperature, two activation energies obtained from electrical modulus spectroscopy studies are similar to that of DC conductivity of impedance plots or AC conductivity at 1 kHz. The activation energies obtained in three different studies are typical value for ionic conductors.

β-Parameter

The electric field relaxation due to ion motion is generally well described by the empirical Kohlrausch function $\Phi(t) = \exp[-(t/\tilde{\imath}_\sigma)^\beta]$ $(0 \le \beta \le 1)$ [22–25]. The $\tilde{\imath}_\sigma$ and β parameters of the stretched exponential function are respectively the conductivity relaxation time and Kohlrausch exponential function. The smaller the value of β, the greater the deviation with respect to Debye-type relaxation. The β parameter is most often interpreted as a result of correlated motions between ions i.e. the jump of a mobile ion in a material can not be treated as an isolated event. It results in a time-dependent motion of other charge carriers in the surroundings. The value of the β parameter becomes smaller as the cooperation between charge carriers is more extended. For very small charge carrier concentrations, the conductivity is essentially characterized by independent jumps, where as when the mobile ion concentration increases, the coupling between charge carriers is more extended.

In both glasses and ionic crystalline ionic conductors, the coupling of charge carriers is reflected by a value β close to 0.5 [25, 26]. It was determined by fitting the circular arc $[Z^{II} = f(Z^{I})]$, the center of

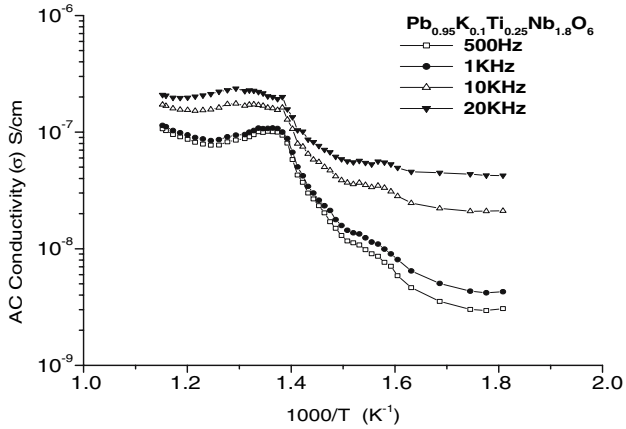

Fig. 10 Variation of AC conductivity with inverse of temperature (K)

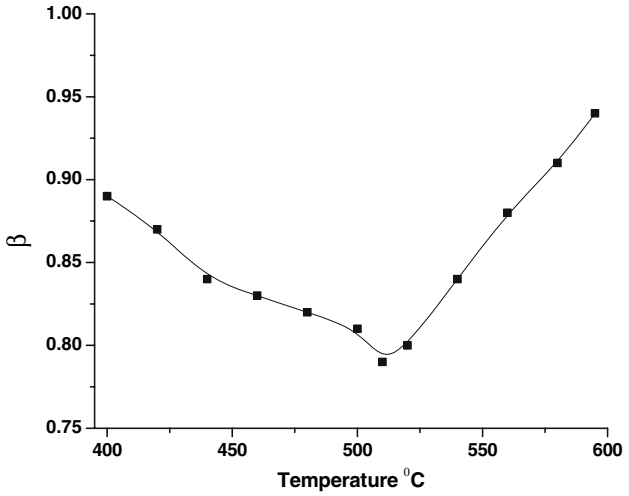

Fig. 11 Stretched exponential parameter β as a function of temperature. Near the phase transition temperature, β has a small value

which is displaced below the real axis. The split allows the determination of the angle Φ and thus β as $\Phi = (1-\beta)\ \pi/2$. Variation of β parameter with temperature in PKTN has been shown in Fig. 11, which covers the transition temperature of the material. The value of β obtained from Z^{II} was 0.79–0.94. Near phase transition temperature, a stretched exponential parameter β as a minimum value 0.79. It implies that distribution of relaxation time in the temperature region has a large width of Φ. From the results of the variation of activation energy and parameter β near phase transition temperature, dynamic process is different from that of apart from phase transition temperature. One can say, according to the lattice dynamics theory, one of the transverse modes (soft-mode) is weakened and the restoring force tends to become zero at the ferroelectric–paraelectric transition [27]. Therefore, if one assumes that the charge carriers couple with the soft-mode, one may expect that the charge carriers become mobile at the phase transition temperature.

Conclusion

(1) The frequency dependency of dielectric, impedance, modulus, and ac conductivity has been studied as a function of temperature. Phase transition temperature 510 °C in PKTN has been found from real dielectric constant versus temperature response.
(2) It is observed that ε^{I} and ε^{II} intersecting only from 350 °C in low frequency (45 Hz) range. There is a sharp raise in ε^{I} and ε^{II} towards low frequency side may be due to conducting ion motion. High value of ε^{I} may be interpreted as accumulation of charge at interface between sample and electrode i.e., space charge polarization.
(3) From Cole–Cole plots high overlapping degree of semi circles suggests that each contribution due to grain and grain boundary presents very similar relaxation frequency.
(4) From the grain resistance, grain boundary resistance and the conduction activation energies of grain and grain boundary, it is concluded that the conducting parameter in PKTN is probably due to grain boundary.
(5) It is evident from the variation of M^{II} with frequency at various temperatures; there is a shift in peak frequencies of M^{II} to higher frequency side as temperature increases. The low frequency side of the peak represents the long-range motion i.e., ions make successful hopping from one site to neighboring site. The high frequency side of M^{II} represents the localized motion of the ions confined to their potential wells.
(6) It is observed that the activation energies obtained from impedance and modulus and ac conductivity studies at 1 kHz in para and ferro regions are typical values for ionic conductors.
(7) From lattice dynamic theory the restoring force tends to become zero at ferro-para electric phase transition due to weakening of soft modes. There fore it is expected that charge carriers become mobile at phase transition temperature.

Acknowledgements Authors K.S. Rao and P. Murali Krishna thanks DRDO—New Delhi, for sanction of a research project and junior research fellowship.

Reference

1. Yamada TY (1975) J Appl Phys 46:2894
2. O'Connell RM (1980) J Appl Phys 49:3324
3. Panday RK, Sridhar U (1983) Ferroelectrics 51:681
4. Oualla M, Zegzouti A, Elaatmani M., Daoud M, Mezzane D, Gagou Y, Saint-gregoire P (2003) Ferroelectrics 29:133
5. Dong M, Raeu JM, Ravez J, Joo G, Hagenmuller P (1995) J Solid State chem 116:185
6. ZhigaoLu, Bonnet JP, Ravez J, Reau JM, Hagenmuller P (1992) J Phys Chem Solids 53:1
7. Hodge IM, Ingram MD, West AR (1976) J Electronal Chem 74:125
8. Jana P, Kallur VA, Drummond MA, Niigli S, Pandey RK (1992) IEEE 374
9. Neurgoanker RR, Oliver JR, Cory WK (1983) Mat Res Bull 18:735
10. SambasivaRao K, Subramanyam ASV, Murali Mohana Rao S (1997) Ferroelectrics 109:215

11. SabasivaRao K, Prasad TNKV, Subramanyam ASV, Lee J-H, Kim J-J, Cho S-H (2003) Mat Sci Engs B 98:279
12. Kim JS, Song TK (2001) J Phys Soc Japan 70:3419
13. Nobre MAL, Lanfredi S (2001) Mater Lett 50:322
14. Nobre MAL, Lan fredi S (2001) J Phys Chem Chem Solids 62:1999
15. Nobre MAL, Lan fredi S (2001) Mater Lett 47:362
16. Cole KS, Cole RH (1941) J Chem Phys 9:341
17. Bauerle JE (1969) J Phys Chem Chem Solids 30:2657
18. Nagai RL, Leon C (1999) Solid State Ionics 125:81
19. Pissis P, Kyritsis A (1997) Solid State Ionics 97:105
20. Shilov VV, Shevchenko VV, Pissis P, Kyritsis A, Georgoussis G, Gommza YuP, Nesin SD, Klimenko NS (2000) J Non-Cryst Solids 275:116
21. Sidebottom DL, Green PF, Brow RK (1995) J Non-Cryst Solids 183:151
22. Williams G, Watts DC (1970) Trans Fraday Soc 23:625
23. Nagai KL, Martin SW (1989) Phys Rev B40:10050
24. Howell FS, Bose RA, Macedo PB, Moynihan CT (1974) J Phys Chem 78:639
25. Reau JM, Rossignol S, Tanguy B, Paris MA, Rojo JM, Sanz J (1995) Solid State Ionics 80:283
26. Zouari N, Mnif M, Khemakhem H, Mhiri T, Daoud A (1998) Solid State Ionics 110:269
27. Zhigao Lu, Bonnet JP, Ravez J, Reau JM, Hagenmuller P (1992) Phys Chem Solids 53:1